iScience

CellPress
OPEN ACCESS

Article

The neutralization of B.1.617.1 and B.1.1.529 sera from convalescent patients and BBIBP-CorV vaccines

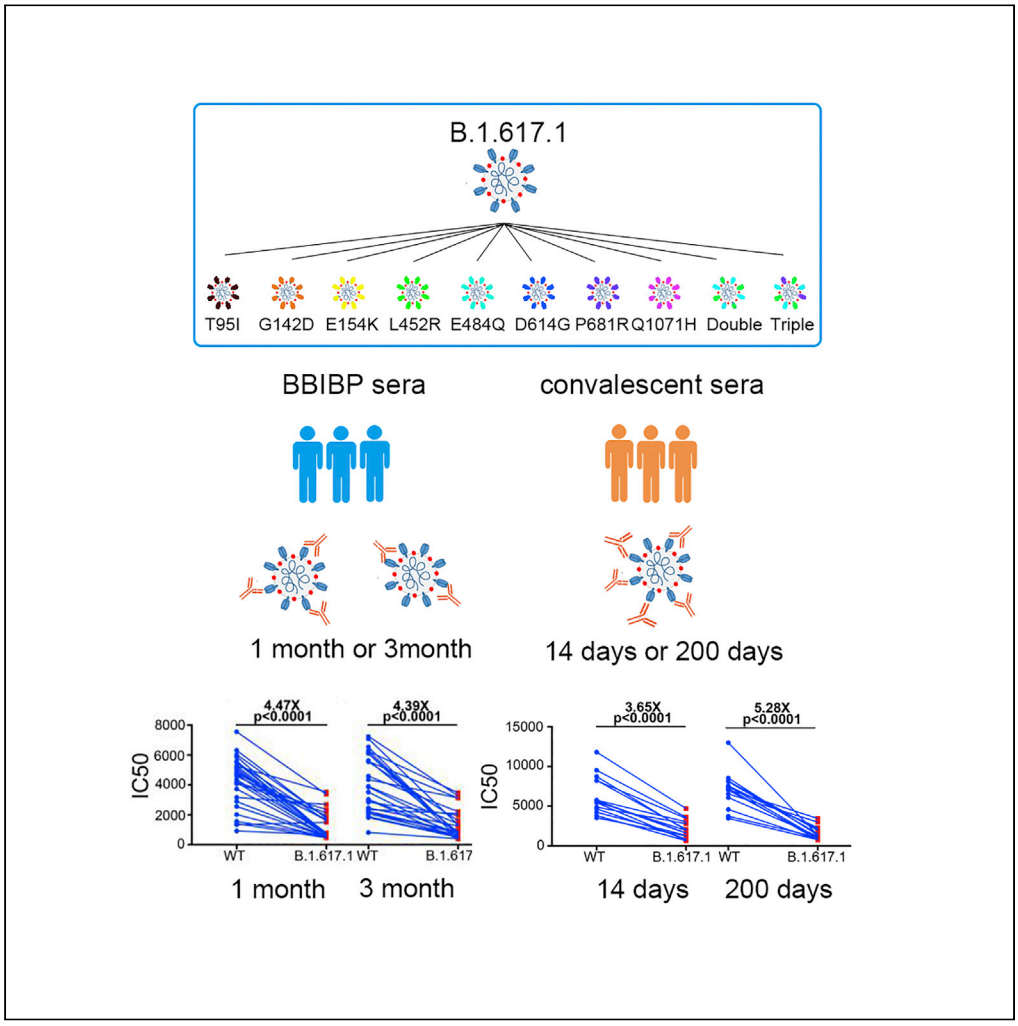

Xinyi Yang, Yuqi Zhu, Jingna Xun, ..., Shibo Jiang, Hongzhou Lu, Huanzhang Zhu

luhongzhou@fuan.edu.cn (H.L.)
hzzhu@fudan.edu.cn (H.Z.)

Highlights

The infectivity of B.1.167.1 is increased by its increased affinity with ACE2

The neutralizing activity of B.1.167.1 and B.1.1.529 is lower than wildtype

The decreased neutralizing activity of B.1.167.1 was mainly caused by E484Q

Yang et al., iScience 25, 105016
September 16, 2022 © 2022
https://doi.org/10.1016/j.isci.2022.105016

iScience

CellPress
OPEN ACCESS

Article

The neutralization of B.1.617.1 and B.1.1.529 sera from convalescent patients and BBIBP-CorV vaccines

Xinyi Yang,[1,7] Yuqi Zhu,[1,7] Jingna Xun,[1,2,7] Jun Liu,[1,3,7] Qing Wen,[1] Yixiao Lin,[4] Xiaoting Shen,[1] Jun Chen,[4] Songhua Yuan,[2] Xiaying Zhao,[1] Jing Wang,[1] Hanyu Pan,[1] Jinlong Yang,[1] Zhiming Liang,[1] Yue Liang,[1] Qinru Lin,[1] Huitong Liang,[1] Chunyan Zhou,[3] Li Jin,[3] Weijian Xie,[3] Jianping Liu,[1] Daru Lu,[1] Tianlei Ying,[5] Yinzhong Shen,[4] Xiaoyan Zhang,[2] Jianqing Xu,[2] Chunhua Yin,[1] Pengfei Wang,[1] Shibo Jiang,[5] Hongzhou Lu,[2,4,6,*] and Huanzhang Zhu[1,8,*]

SUMMARY

The SARS-CoV-2 variants B.1.617.1 (Kappa) contain multiple mutations in the spike protein. However, the effect of B.1.617.1 lineage-related mutants on viral infectivity and inactivated-virus vaccine efficacy remains to be defined. We therefore constructed 12 B.1.617.1-related pseudoviruses and systematically studied the effects of mutations on virus infectivity and neutralization resistance to convalescent and inactivated virus vaccine sera. Our results show that the B.1.617.1 variant exhibited both higher infectivity and neutralization resistance in sera at 1 or 3 months after vaccination of 28 individuals and at 14 and 200 days after discharge of 15 convalescents. Notably, 89% of vaccines and 100% of the convalescent serum samples showed more than 2.5-fold reduction in neutralization against one single mutation: E484Q. Besides, we found a significant decrease in neutralizing activity in convalescent patients and BBIBP-CorV vaccines for B.1.1.529. These findings demonstrate that inactivated-virus vaccination or convalescent sera showed reduced, but still significant, neutralization against the B.1.617.1 variant.

INTRODUCTION

The COVID-19 pandemic has already lasted for more than a year, but new infections are still escalating throughout the world (Wu et al., 2020; Zhou et al., 2020). Although mRNA-, viral vector-, protein- and inactivated-virus-based COVID-19 vaccines have been deployed globally, a major concern is the emergence of SARS-CoV-2 variants of concern (VOC) and variants of interest (VOI) (Gupta, 2021). These variants with mutations in the spike protein have a strong influence on SARS-CoV-2 transmission, antibody resistance and vaccine efficacy, essentially because the spike protein is critical for viral entry. Many mutations reside in the antigenic supersite in N-terminal domain (NTD) (Cerutti et al., 2021; Harvey et al., 2021; McCallum et al., 2021) or in the ACE2-binding site which are the major targets of potent virus-neutralizing antibodies (Piccoli et al., 2020). Three independent SARS-CoV-2 VOCs, B.1.1.7 (Alpha) (Galloway et al., 2021; Volz et al., 2021a,2021b), B.1.351 (Beta) (Tegally et al., 2020, 2021), and P.1 (Gamma) (Faria et al., 2021) have emerged. Indeed, several groups have revealed that the B.1.1.7, B.1.351, P.1, and B.1.167.2 (delta) variants are differentially resistant to the neutralizing antibodies elicited in convalescent and vaccinated individuals (Chen et al., 2021; Collier et al., 2021; Edara etal., 2021; Garcia-Beltran et al., 2021; Liu et al., 2021a, 2021b; Mlcochova et al., 2021; Wang et al., 2021a, 2021b). These variants are known to possess multiple mutations across the genome, including several in the S protein, such as E484K, N501Y, and K417 N/T (Leung et al., 2021; Rambaut et al., 2020; Volz et al., 2021a,2021b). The E484K mutation, initially identified in B.1.351 and subsequently appearing in B.1.1.7 and P.1 strains, helps the virus to escape immune response, and thus higher level of neutralizing antibodies are required to prevent infection from B.1.1.7 variants with E484K (Wise, 2021). Structurally, the E484K mutation results in a spike protein side chain charge change, preventing salt bridge formation and allowing escape from some monoclonal antibodies (Zhou et al., 2021). The N501Y mutation, which exists in all B.1.1.7, B.1.351, and P.1 variants, was found to enhance the affinity between RBD and ACE2 by about 7-fold compared to wildtype (WT). This leads to enhanced

[1]State Key Laboratory of Genetic Engineering and Engineering Research Center of Gene Technology, Ministry of Education, Institute of Genetics, School of Life Sciences, Fudan University, Shanghai 200438, China

[2]Scientific Research Center, Shanghai Public Health Clinical Center, Fudan University, Shanghai, China

[3]Fubio (Suzhou) Biomedical Technology Co., Ltd, Suzhou, China

[4]Department of Infectious Diseases and Immunology, Shanghai Public Health Clinical Center, Fudan University, Shanghai, China

[5]Key Laboratory of Medical Molecular Virology (MOE/NHC/CAMS), School of Basic Medical Sciences, Fudan University, Shanghai, China

[6]The Third People's Hospital of Shenzhen, Shenzhen, China

[7]These authors contributed equally

[8]Lead contact

*Correspondence: luhongzhou@fuan.edu.cn (H.L.), hzzhu@fudan.edu.cn (H.Z.)

https://doi.org/10.1016/j.isci.2022.105016

viral transmission, but not increased virulence (Liu et al., 2021b). This mutation can also decrease the efficacy of some monoclonal antibodies, supporting the therapeutic use of antibody cocktails (Zhou et al., 2021). Mutations at K417 increase the affinity of the RBD to ACE2, increase chances of immune escape, and reduce monoclonal antibody response and convalescent plasma-mediated neutralization (Wu et al., 2021). K417N and K417T RBD mutations have been identified in B.1.351 and P.1, respectively. In combination with their common E484K and N501Y mutations, K417 alterations induce a relatively large conformational change that may increase the potential for immune escape (Nelson et al., 2021). The more recently identified SARS-CoV-2 variants, B.1.617.1 (Kappa) and B.1.617.2 (Delta), are more infectious and virulent compared to the original wild-type virus (Cherian et al., 2021). The World Health Organization has designated the B.1.617.1 lineage as a variant of interest (VOI). The B.1.617.1 variant contains several mutations within the spike protein, including some in the N-terminal antigenic supersite (G142D and E154K), in the receptor binding domain (L452R and E484Q) and in the polybasic furin cleavage site at the S1/S2 boundary (P681R). A new variant with two mutations, E484Q and L452R, and initially reported in India was named as a "double mutant". This new variant is believed to be creating the latest wave of infections in India in 2021, making it the second most affected country in the world, surpassing Brazil. Recent studies have shown that the B.1.617.1 variant is resistant to mRNA vaccine-induced NAbs (Edara et al., 2021; Liu et al., 2021a). However, the effect of B.1.617.1 on viral infectivity and inactivated virus vaccine efficacy remains to be defined. We therefore analyzed the infectivity of 12 pseudotyped viruses displaying spike proteins derived from WT, the B.1.617.1 variant and its single mutations, double mutations (L452R/E484Q) or triple mutations (L452R/E484Q/P681R) in SARS-CoV-2-susceptible cell lines and HEK293T cells expressing ACE2. We also evaluated the resistance of these pseudoviruses to neutralization using convalescent sera from 15 convalescent volunteers infected with coronavirus disease 2019 (COVID-19) obtained 14 days and 200 days after recovery and sera from 28 participants obtained 1 month and 3 months after receipt of the second dose of inactivated-virus vaccine, BBIBP-CorV (Sinopharm), which was developed in China.

RESULTS

Construction of the pseudotyped viruses related to B.1.617.1

The B.1.617.1 variant was initially described in India in October 2020 (GISAID ID: EPI_ISL_1372093). It contains 8 mutations within the spike protein (T95I, G142D, E154K, L452R, E484Q, D614G, P681R, and Q1071H) (Figure 1A). To study the effects of B.1.617.1-related mutations, we generated a total of 12 pseudotyped lentiviruses containing the spikes of wild-type Wuhan-1 reference strain (WT), each of the individual mutations, and those with all 8 mutations or double mutations (L452R/E484Q) or triple mutations (L452R/E484Q/P681R) of the B.1.617.1 variant (Figure 1B). These pseudoviruses were prepared as described in STAR Methods, and each was found to have a robust titer (Figure S1).

Infectivity of the B.1.617.1-related variants

We generated 293T cells expressing the SARS-CoV-2 receptor ACE2 (293T-hACE2). ACE2 expression was monitored using Western blot and flow cytometry (Figure S2). We first investigated the potential infection-related effects of these mutations in assays with three cell lines known to be susceptible to SARS-CoV-2 pseudotyped virus infection: Huh-7-, Calu-3- and 293T-hACE2. Compared to WT pseudovirus, our findings demonstrate that the B.1.617.1 variant displayed a 3-3.5-fold increase in infectivity in all three cell lines (Figure 1C), whereas no significant difference was found between the B.1.617.1 and D614G variants. Moreover, the pseudotyped viruses carrying some of the single mutations (L452R, E484Q, D614G, P681R) or double (L452R/E484Q) or triple (L452R/E484Q/P681R) mutations exhibited a 2- to 4-fold increase in infectivity compared to WT, whereas no significant increase in infectivity was observed in these cell lines for the other single point mutations (T95I, G142D, E154K, and Q1071H) (Figure 1C), and when the single (L452R), double (L452R/E484Q), and triple (L452R/E484Q/P681R) mutations are combined with D614G, the infectivity of double (L452R/E484Q) and triple (L452R/E484Q/P681R) mutations is also slightly increased compared with that of the D614G mutation alone (Figure S3), which suggesting that the single mutants (L452R, E484Q, D614G, and P681R) and double (L452R/E484Q) and triple (L452R/E484Q/P681R) mutations may contribute to SARS-CoV-2 infectivity.

Effect of the B.1.617.1 variant on the binding affinity to ACE2 and membrane fusion

The 8 mutations in the spike protein of the B.1.617.1 variant are mapped on a structure of the spike protein (Figure 2A). To directly assess the effect of these mutations on the binding affinity to ACE2, the spike proteins of B.1.617.1-related variants were expressed and purified for binding affinity assay. Our findings

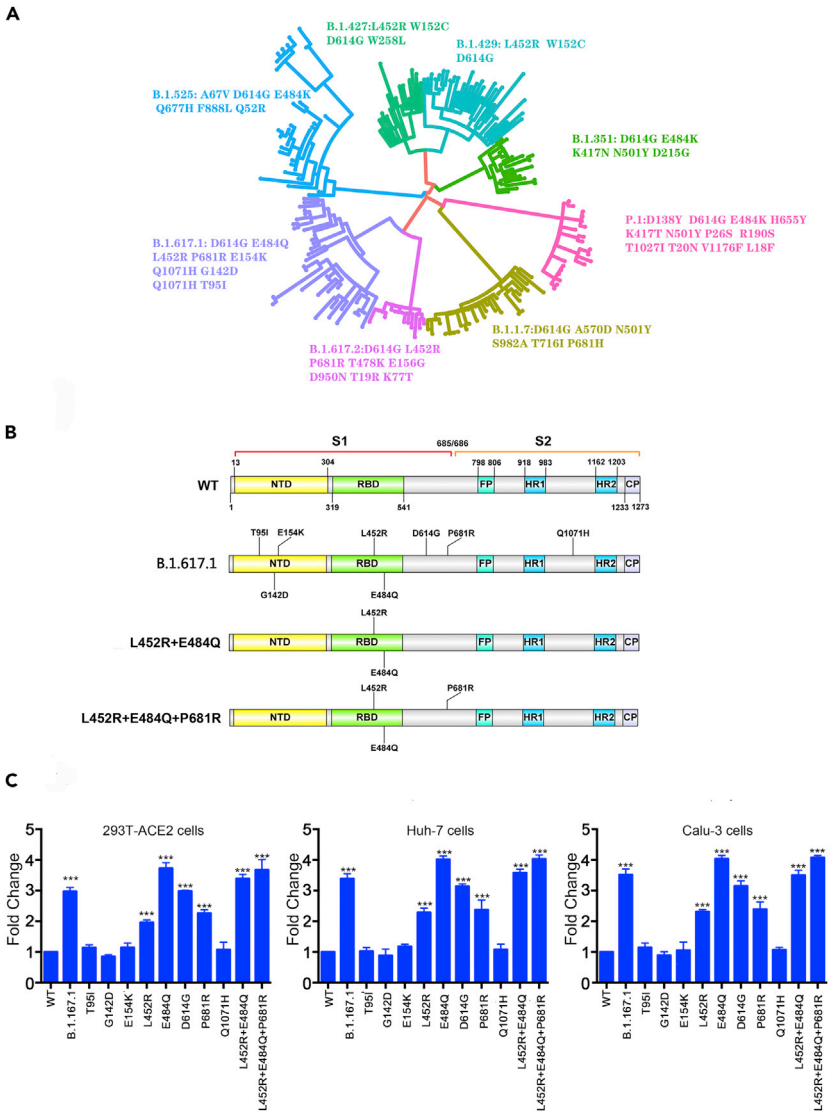

Figure 1. Infectivity of variant spike protein pseudotyped virus

(A) Phylogenetic tree of SARS-CoV-2 variants.

(B) Mutations in the viral spike identified in SARS-CoV-2(WT), B.1.617.1, L452R + E484Q strain, and L452R + E484Q + P681R strain.

(C) 293T-ACE2, Huh-7, Calu-3 cell lines were infected with pseudotyped viruses with 12 strains. The infected cell lysates were analyzed by RLU. The results were represented by ratio of WT to variants. All experiments were performed with 3 duplications independently (mean ± SEM).

demonstrate that the B.1.617.1 variant significantly increased the binding affinity to human ACE2 compared to WT. D614G itself did not cause an increase in ACE2 binding compared to WT; however, spike proteins containing the single L452R or E484Q mutation, as well as those with double mutations (L452R/E484Q) or triple mutations (L452R/E484Q/P681R), showed a significant increase in ACE2-binding compared to D614G (Figure 2B). To characterize which amino acid change in the spike protein of B.1.617.1 is responsible for its enhanced cleavage, pseudoviruses with each of the variant spike proteins were lysed, and western blot showed that the level of cleaved S2 subunit was significantly increased by the B.1.617.1 variant or single P681R or triple mutations with P681R (Figure 2C). This suggests that P681R alone is responsible for the enhanced S cleavage seen in the pseudoviruses of B.1.617.1 lineages. To investigate which amino acid change in the spike protein of B.1.617.1 is responsible for syncytia formation, 293T-hACE2 was infected by pseudoviruses with each of the variant spike proteins. Microscopic

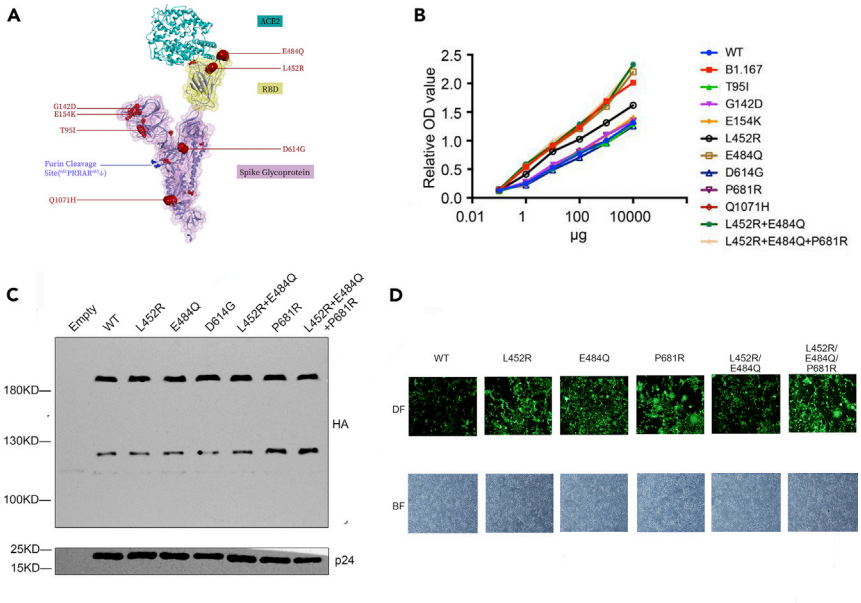

Figure 2. Biological characteristics of different point mutations in B.1.167.1 strain

(A) B.1.167.1 S protein and ACE2 protein molecular interaction diagram. Different point mutation positions are marked and displayed. The ACE2 protein is represented in green. The RBD region of the S protein is represented by yellow, and the spike glycoprotein region is represented by purple.

(B) Analysis of the effect of different point mutations, double mutations, triple mutations and B.1.167.1 variant on the affinity of S and ACE2. ACE2 protein was coated as an antigen in a 96-well plate, incubated with S protein with different mutations, and then anti-HA was used as the primary antibody for ELISA detection.

(C) Analysis of different point mutations and B.1.167.1 cleavage of S1 and S2 subunits of S protein. S protein was determined by western blot of whole pseudotyped virus lysate with anti-HA antibody.

(D) Analysis of the effect of different point mutations and B.1.167.1 variant on cell fusion. After 72 h of infection of 293T-ACE cells with different strains, cell morphology was observed by fluorescence microscopy.

observations showed that the B.1.617.1 variant significantly increased syncytia formation compared to WT (Figure 2D). Notably, only single P681R and triple mutations with P681R showed a significantly increased fusion efficacy compared to WT (Figure 2D). These results suggest that the B.1.617.1 lineages can form syncytia, mostly attributable to the P681R mutation.

Reduced neutralization activity of vaccine sera

To compare the protective effect of the inactivated vaccine against the wild-type SARS-CoV-2 and the B.1.167.1 variant, we conducted a neutralization experiment to detect whether the neutralizing antibody could be induced and whether protection could be effectively established. We serially diluted the serum samples collected from 28 volunteers at 2 different time points (average 1 month and 3 months after vaccination) (Table 1). Then we detected the neutralizing effect of antibodies in the plasma using a luciferase-expressing lentiviral pseudotype system. Each vaccine's serum sample was assayed for neutralization against B.1.617.1 and WT viruses. Every sample from both the 1-month and the 3-month time points showed neutralizing activity against B.1.617.1 or WT viruses, but the activity against B.1.617.1 was lower compared to that of WT (Figures 3A and 3B) (Figures S4 and S5). To determine which amino acid change in the spike protein of B.1.617 is responsible for the reduction of neutralizing activity, we used pseudoviruses with 8 single mutations, or double mutations (L452R/E484Q) or triple mutations (L452R/E484Q/P681R) to perform the antibody neutralization experiment. The neutralization curves are presented in Figures S3 and S4. The results are quantified and tabulated as fold increase or decrease in neutralization IC_{50} titers relative to the WT, and a summary can be found in Figure 3B. Relative to neutralization of WT virus, it can be seen that the neutralization of some (L452R, E484Q, P681R), but not other single mutations (T95I, G142D, E154K, D614G, Q1071H), was reduced in most serum samples. Especially 89% (25/28) of the serum samples from both 1 and 3 months after vaccination had more than 2.5-fold reduction in neutralizing activity against the single mutation E484Q (Figure 3B), indicating that E484Q in B.1.617.1 has an

Table 1. Characteristics of study subjects

Characteristics of study subjects		
Characteristics	COVID-19 convalescent patients	BBIBP-CorV inocultors
Number of volunteers	15	28
Age(median,range)	53(33-68)	29.5(22-56)
Gender		
Male(%)	6(40%)	14(50%)
Female(%)	9(60%)	14(50%)
Blood sampling interval(median,range) 1st	14.5(9-19)	37.5(19-47)
Blood sampling interval(median,range) 2nd	200.5(189-229)	91(75-100)
Clinical classification		
Severe	1	NA
Non-severe	14	NA

Age, sex, sampling interval, and clinical diagnostic information were included for 15 convalescent patients and 28 inactivated-virus vaccines.

appreciable impact on the neutralizing activity of vaccines' serum. The double mutations (L452R/E484Q) or triple mutations (L452R/E484Q/P681R) also have an appreciable impact on the neutralizing activity of vaccines' serum. The extent of the decline in neutralizing activity is more evident in Figures 3C–3F. Compared to WT, the pseudoviruses with B1.617.1, double mutations (L452R/E484Q) or triple mutations (L452R/E484Q/P681R) showed a significant decrease in the neutralizing activity of vaccines' sera from both 1 and 3 months (Figures 3C and 3D). The neutralizing activity against the wild-type SARS-CoV-2 or B.1.617.1, or double mutations (L452R/E484Q), or triple mutations (L452R/E484Q/P681R) was essentially unchanged when comparing vaccines' serum from the 1-month and 3-month time points (Figures 3E and 3F). Besides, in addition to the mutations near the RBD, we further explored whether the three mutations (T95I/G142D/E154K) in the NTD region are synergistically resistant to neutralization by 10 vaccines randomly selected. The results showed that the neutralizing activity of pseudoviruses containing mutations in the three NTD regions decreased by 1.66 times and 1.87 times compared with WT, respectively, but there was no significant statistical difference (Figure S6).

Reduced neutralizing activity of COVID-19 convalescent plasma

To evaluate the neutralizing activity of COVID-19 convalescent plasma against the B.1.167.1 variant, we collected plasma samples from 15 convalescent volunteers obtained from Shanghai Public Health Clinical Center at 2 different times (average 14 days and 200 days) (Table 1). Similar to inactivated-virus vaccine sera, we found that plasma samples from all convalescent volunteers had neutralizing activity against WT or the B.1.167 variant (Figures 4A and S7). These results are summarized as fold increase or decrease in plasma neutralization IC_{50} titers in Figure 4B. Every plasma sample was also tested against each mutant pseudovirus, and those findings are shown in Figure S7 and summarized in Figures 4B and 4C. We found that mutations in the RBD region, including L452R and E484Q, as well as the P681R mutation near the furin splice site, significantly reduced the neutralizing activity of plasma from COVID-19 convalescent volunteers (Figure 4B). It is particularly worth noting that 100% (15/15) of the serum samples collected at either 14 or 200 days had more than 2.5-fold reduction in neutralizing activity against the single mutation E484Q (Figure 4B). For point mutations in non-RBD regions, including T95I, G142D, E154K, and Q1071H, the neutralizing activity of IC_{50} did not demonstrate any significant change compared to the WT strain (Figures 4B and S7). However, we did find that the IC_{50} of neutralizing activity against the B.1.617.1 variant was reduced by 3.65-fold and 5.28-fold compared to WT for the 14-day and 200-day time points, respectively (Figures 4B and 4C). Compared to WT, the pseudoviruses with double mutations (L452R/E484Q) or triple mutations (L452R/E484Q/P681R) were shown to significantly decrease the neutralizing activity of convalescent plasma from 14 or 200 days (Figures 4B and 4D). The neutralizing activity against the wild-type SARS-CoV-2 or B.1.617.1 was significantly reduced in sera from convalescent volunteers between 14 and 200 days (Figures 4C and 4D). Finally, we analyzed the neutralizing activity of the same variant at different time points. For WT, the B.1.617.1 variant and triple mutations (L452R/E484Q/P681R), we found that the IC_{50} of neutralizing activity in the convalescent volunteers' plasma decreased significantly over

A

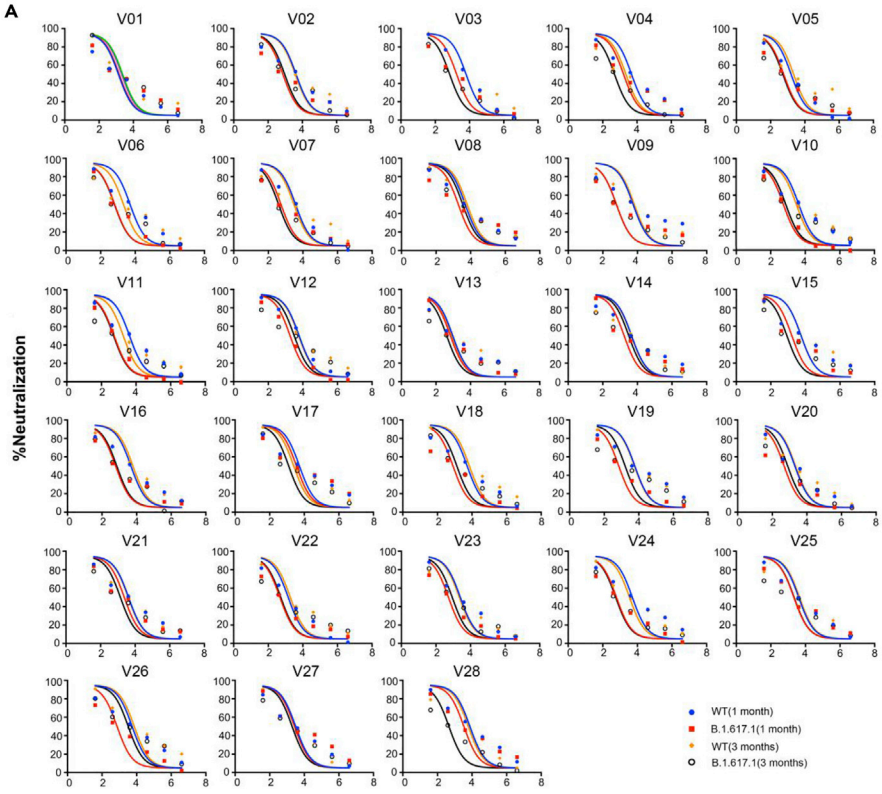

B

Fold change	IC50 of WT / IC50 of Variants																					
	WT/B.1.617.1		WT/T95I		WT/G142D		WT/E154K		WT/L452R		WT/E484Q		WT/D614G		WT/P681R		WT/Q1071H		WT/L452R +E484Q		WT/L452R+ E484Q+P681R	
Volunteer	1 M	3 M	1 M	3 M	1 M	3 M	1 M	3 M	1 M	3 M	1 M	3 M	1 M	3 M	1 M	3 M	1 M	3 M	1 M	3 M	1 M	3 M
V01	0.89	1.13	0.60	1.12	0.95	2.40	0.89	3.67	1.39	4.31	2.48	5.35	1.45	2.36	1.86	4.05	1.06	2.12	2.78	8.00	2.48	8.27
V02	5.92	4.12	1.38	1.36	0.99	0.94	1.01	1.06	7.15	7.95	12.46	13.13	0.78	1.09	3.79	3.55	1.07	0.88	8.05	7.30	8.60	8.94
V03	3.55	9.04	1.16	1.33	1.46	1.02	1.65	1.53	3.45	9.23	9.59	11.32	0.89	9.38	2.96	4.06	1.16	1.22	8.47	8.90	8.21	11.35
V04	2.92	4.63	1.16	0.69	1.39	0.67	1.44	0.45	3.63	4.04	6.88	4.11	1.12	1.54	2.49	2.76	0.77	1.10	7.28	4.21	5.39	5.30
V05	2.70	4.23	0.81	1.55	1.18	1.11	0.65	1.64	1.90	3.31	2.77	6.54	0.70	1.36	1.92	2.42	0.54	0.64	3.24	4.57	3.46	5.30
V06	7.73	3.32	1.09	1.07	1.12	1.40	0.98	1.62	5.18	3.46	10.99	5.40	3.13	2.16	4.70	2.99	2.36	0.91	4.02	4.21	9.47	4.04
V07	6.96	7.74	0.86	1.02	0.70	1.05	0.61	1.24	8.44	6.46	10.64	10.30	0.98	1.65	4.70	4.20	1.34	1.23	13.15	9.43	12.97	6.70
V08	2.51	1.79	1.10	1.35	1.25	0.92	1.00	0.87	1.67	3.47	4.11	9.95	1.17	1.47	1.56	5.92	1.14	1.20	2.61	7.69	1.71	8.21
V09	9.17	10.86	1.79	0.88	1.22	1.24	1.30	0.97	5.66	2.07	12.10	10.12	1.23	1.59	6.74	6.10	1.18	1.69	19.54	14.33	15.88	13.82
V10	7.75	4.10	1.05	1.31	0.97	1.84	0.58	1.31	7.27	3.09	8.61	5.23	1.55	2.46	5.07	3.72	1.19	2.79	7.48	4.83	6.99	4.91
V11	5.26	3.63	1.09	0.79	1.25	0.66	1.59	0.87	3.68	2.96	5.14	5.55	1.59	1.02	3.87	1.64	0.85	0.54	10.05	5.22	7.04	3.87
V12	3.34	1.78	1.12	1.13	0.90	0.76	0.73	1.07	3.55	1.58	4.70	13.60	1.14	1.46	2.33	1.39	1.25	1.33	7.13	10.05	11.11	9.17
V13	1.36	2.00	0.37	0.91	0.53	0.90	1.05	0.95	1.46	1.50	2.02	1.55	1.53	1.36	1.20	0.99	0.66	0.65	2.89	1.47	2.24	1.69
V14	2.70	1.39	0.72	0.99	1.04	1.05	1.02	1.19	3.14	1.75	7.78	4.15	1.32	1.36	2.44	1.50	0.69	0.91	6.66	3.38	7.03	3.16
V15	3.41	6.73	1.69	1.09	0.79	0.86	0.99	0.88	4.69	3.35	6.64	8.47	1.72	1.43	2.33	2.55	1.20	1.01	9.40	7.64	13.34	6.69
V16	7.69	8.55	0.59	1.10	0.95	1.24	0.62	1.20	6.66	2.14	10.09	10.47	1.47	1.81	5.05	2.01	0.89	1.60	12.16	12.11	9.21	10.91
V17	1.49	1.95	0.76	1.24	0.71	1.71	0.73	2.04	1.32	1.31	3.06	2.97	2.17	1.22	1.01	2.46	1.26	1.33	3.19	3.32	14.60	2.71
V18	6.58	5.31	1.40	1.19	1.33	1.09	0.99	1.55	5.02	4.43	9.23	8.63	1.32	1.54	1.99	2.10	0.76	1.17	6.26	1.94	10.53	4.28
V19	8.48	3.43	1.35	1.22	1.26	0.93	0.66	0.37	3.12	2.49	6.34	3.30	2.12	1.37	10.13	1.62	0.86	1.52	13.47	1.82	3.82	1.40
V20	4.18	2.85	0.67	0.98	0.62	2.63	0.45	1.75	3.64	2.38	2.06	3.00	3.43	1.51	2.64	2.23	0.80	2.45	4.13	2.46	2.60	2.31
V21	1.77	2.79	1.09	0.94	2.05	0.73	1.09	0.72	1.46	2.29	2.84	5.62	2.80	1.62	2.25	1.42	1.62	0.87	2.44	3.36	12.00	5.44
V22	3.02	3.56	0.91	1.29	0.84	1.29	0.30	1.19	2.07	2.04	3.30	3.35	1.12	2.23	2.43	3.38	0.84	1.37	2.05	3.00	0.93	2.92
V23	4.88	2.56	1.12	0.80	1.13	0.91	0.77	0.70	3.09	2.63	4.92	5.28	2.23	2.32	2.28	2.57	1.45	0.72	5.69	3.47	3.28	3.79
V24	8.28	6.31	1.24	1.17	0.78	1.11	0.98	0.97	7.14	5.73	8.81	6.88	1.47	1.38	9.69	5.07	1.22	1.28	5.88	5.62	13.57	5.92
V25	1.90	2.07	1.14	1.01	1.37	1.17	1.62	1.04	1.25	2.34	4.14	7.02	1.66	1.36	4.29	1.87	1.04	1.16	5.07	5.33	5.16	5.95
V26	7.43	2.22	1.08	1.46	0.93	1.09	0.59	0.95	9.46	2.02	13.75	12.53	1.52	2.14	10.67	2.42	1.74	1.79	4.70	6.70	3.43	5.80
V27	1.17	1.45	1.83	1.51	0.76	1.02	0.94	1.08	1.31	1.41	3.01	3.84	2.18	1.15	0.97	1.37	0.88	0.83	2.74	2.75	2.79	2.58
V28	2.24	13.26	1.03	1.17	1.48	1.30	0.88	1.28	1.93	2.47	6.83	12.00	2.44	1.55	2.52	2.47	1.14	1.15	5.62	5.24	5.07	5.65

C

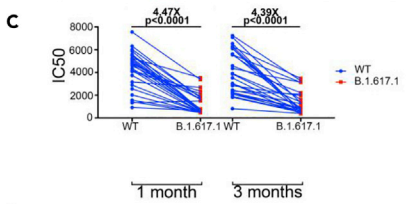

D

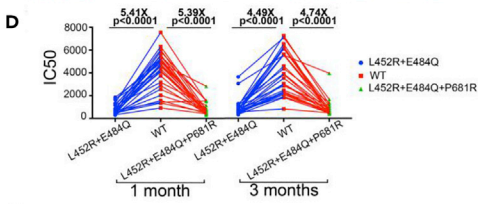

E

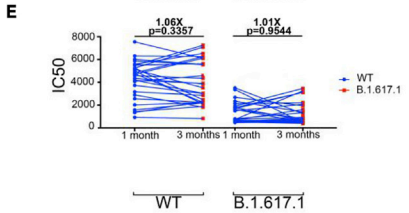

F

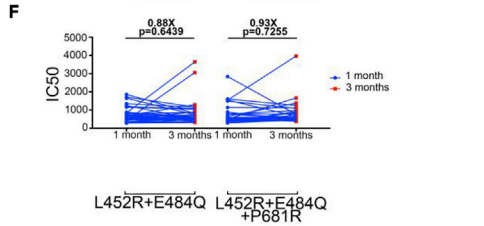

Figure 3. B.1.617.1, L452R, E484Q, L452R + E484Q, and L452R + E484Q + P681R pseudoviruses are more resistant to neutralizing antibody of inactivated-virus vaccine vaccines

(A) Neutralization assay results of 28 vaccines (V01-V28) against WT and B.1.617.1 at 1 and 3 months after inoculation. All data were obtained from three independent experiments (mean ± SEM). The X axis is log10, which represents the plasma dilution ratio, and the Y axis, which represents the protective efficacy of neutralizing antibody.

(B) Ratios of IC_{50} of WT to IC_{50} of all 12 variants of 1 and 3 months represented as a heatmap with darker color implying greater change (≥2.5-fold).

(C) Change in plasma neutralization IC_{50} values of 28 vaccines from WT to B.1.617.1 at 1 and 3 months after vaccination, respectively.

(D) Change in plasma neutralization IC_{50} values of 28 vaccines from WT to L452R + E484Q and L452R + E484Q + P681R at 1 and 3 months after vaccination, respectively.

(E) Change in plasma neutralization IC50 values of 28 vaccines at 1 to 3 months after vaccination for WT and B.1.617.1, respectively.

(F) Change in plasma neutralization IC_{50} values of 28 vaccines at 1 to 3 months after vaccination for L452R + E484Q and L452R + E484Q + P681R, respectively. Mean fold changes in IC_{50} values are written above the p values. Statistical analysis was performed using a paired *t*-test. $P < 0.05$ was considered statistically significant.

time (WT: $p = 0.005$, B.1.617.1: $p = 0.0026$, and triple mutations: $p = 0.0326$) (Figures 4E, 4F, and S7), which is different from what we saw for the vaccines' sera (Figure 4F). Like the vaccines sera, we also randomly selected 10 convalescent sera as samples to further explore the changes in the neutralizing activity of pseudoviruses containing mutations in the three NTD regions. The results showed that, like the vaccinated, the neutralizing activity of the sera of the convalescents against the NTD mutation was 1.16 and 1.31 times lower than that of the wildtype, respectively, but there was no statistical difference (Figure S6).

Reduced neutralization activity of vaccine sera and COVID-19 convalescent plasma for B.1.1.529

Given that the main virus strain in the world was B.1.1.529, and B.1.1.529 also contains the mutation of amino acid 484. Therefore, we also want to use our pseudovirus reporting system to explore neutralization activity of vaccine sera and COVID-19 convalescent plasma for B.1.1.529. We detected the neutralizing effect of antibodies in the plasma and found that every sample from both the 1-month and the 3-month time points showed neutralizing activity against B.1.1.529 had more than −4.16 or −7.18-fold reduction compared to that of WT (Figures 5A and 5B). Similarly, for a random selection of 10 recovered patients, at different time points, there were also similar results (Figures 5C and 5D). Combined with our B.1.617.1 results, we speculate that the E484A mutation also leads to a significant immune evasion effect of the B.1.1.529 strain.

DISCUSSION

The recent surge in COVID-19 cases and deaths in India is paralleled by the spread of the novel SARS-CoV-2 variant B.1.617.1. This variant harbors mutations in the spike protein that might alter important biological properties of the virus, including the efficiency of entry into target cells and the degree of vaccine protection. Here, we constructed 12 B.1.617.1-related pseudoviruses using a lentivirus-based system and systematically studied the effects of mutations on virus infectivity and neutralization resistance to convalescent plasma and inactivated-virus vaccine sera. Compared with the Wuhan-1 reference variant, we found that the B.1.617.1 variant exhibited both higher infectivity and efficient neutralization resistance. In this study, we also determined which of the B.1.617.1 mutations within the spike protein or their combinations contribute to this enhanced infectivity and neutralization resistance. Relative to wild-type SARS-CoV-2, we found that pseudoviruses carrying single mutants (L452R, E484Q, D614G, and P681R) and double (L452R/E484Q) and triple (L452R/E484Q/P681R) mutations are highly infectious which could be associated with significantly increased binding affinity between these mutations and ACE2. On the contrary, Ferreira et al. reported that B.1.617.1 spike bearing L452R, E484Q, and P681R mediates entry into cells with only slightly reduced efficiency compared to Wuhan-1 (Ferreira et al., 2021). A recent report using a spike B.1.617.1 with a larger set of mutations found variable entry efficiency relative to wildtype across cell types (Ferreira et al., 2021). The reason for the inconsistent results could be related to several factors, such as different infected cells, virus titer and time to assay after pseudovirus infection.

Nonetheless, in the present study, we found that samples from both vaccines and convalescents acquired neutralizing activity against WT and B.1.617.1 and that the corresponding protective effect lasted for at least 3–6 months. This reminds us that vaccination with inactivated-virus vaccine is an effective way to fight

A

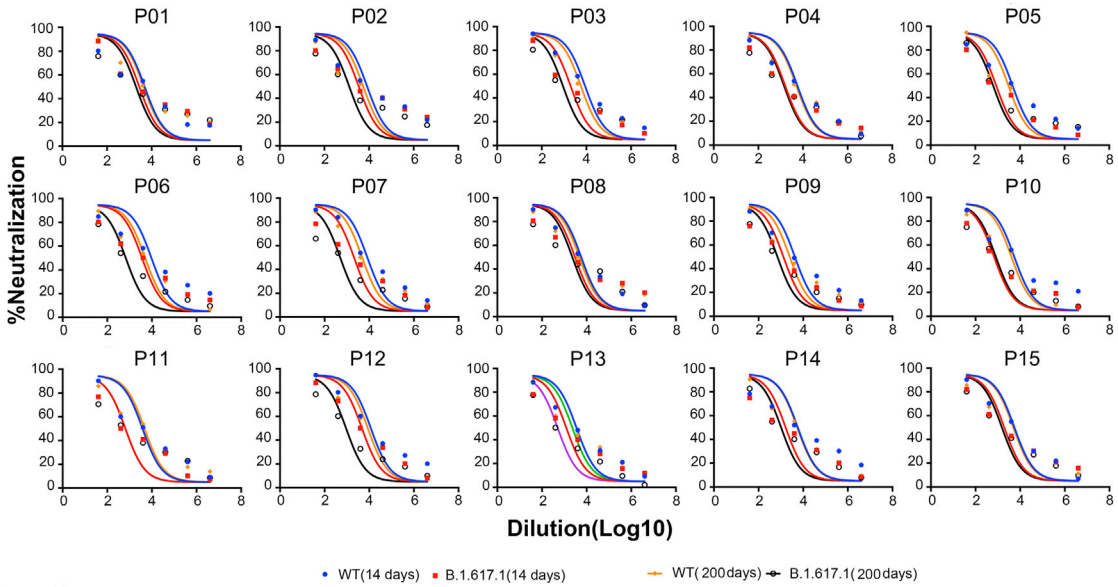

B

Fold change	IC50 of WT / IC50 of Variants																					
	WT/B.1.617.1		WT/T95I		WT/G142D		WT/E154K		WT/L452R		WT/E484Q		WT/D614G		WT/P681R		WT/Q1071H		WT/L452R+ E484Q		WT/L452R+ E484Q+P681R	
Volunteer	14 D	200 D	14 D	200 D	14 D	200 D	14 D	200 D	14 D	200 D	14 D	200 D	14 D	200 D	14 D	200 D	14 D	200 D	14 D	200 D	14 D	200 D
P01	1.74	2.19	0.96	1.09	0.96	1.00	0.85	1.13	1.61	2.01	2.92	4.74	1.35	1.89	1.77	1.51	0.99	0.85	3.18	3.03	2.42	5.21
P02	2.37	4.20	0.87	0.88	1.07	0.78	0.97	0.81	2.42	2.63	5.83	8.74	1.65	3.22	2.73	2.02	1.11	0.83	5.34	8.46	7.67	8.31
P03	4.45	6.38	1.14	1.01	1.61	1.19	1.37	1.18	5.86	1.81	9.29	4.26	2.26	1.51	6.67	2.51	1.33	1.20	11.76	4.29	9.81	3.05
P04	3.52	3.56	0.82	1.05	0.77	1.04	0.95	1.05	2.16	1.73	6.75	8.28	1.50	1.44	4.49	6.89	1.02	0.96	4.68	4.97	4.67	5.58
P05	5.39	5.74	1.11	1.08	1.09	1.50	0.81	1.63	3.83	4.31	7.54	6.74	1.27	2.57	4.19	4.79	1.05	1.32	6.86	5.50	6.59	5.38
P06	2.63	7.42	0.96	0.87	0.98	0.86	1.46	0.80	1.79	6.90	5.28	11.31	1.35	1.94	2.43	6.84	1.50	0.83	12.42	7.96	7.81	6.41
P07	3.94	9.64	1.10	1.02	1.17	1.01	1.23	1.10	2.30	6.68	3.65	9.92	1.39	1.35	2.14	4.75	1.24	0.93	2.89	5.69	2.60	5.00
P08	1.90	2.05	1.05	1.04	1.14	0.89	1.20	1.07	1.86	1.23	7.11	3.41	1.24	0.95	1.81	1.24	1.11	1.20	4.51	2.34	4.13	2.43
P09	3.25	3.54	1.01	1.03	0.91	0.85	0.94	0.88	1.74	3.05	6.93	4.00	1.02	1.37	2.12	2.35	1.06	0.96	4.61	2.76	2.40	3.32
P10	8.03	5.00	1.18	1.12	0.94	0.98	1.36	0.95	4.03	3.68	8.99	6.70	1.35	1.09	1.26	4.23	1.00	1.13	6.57	5.83	4.12	5.35
P11	5.86	7.19	0.85	1.24	0.81	0.86	0.83	0.98	1.41	2.30	6.40	9.92	1.26	1.46	4.04	2.27	0.86	1.07	4.65	7.18	4.97	7.23
P12	2.51	9.47	1.04	1.49	1.08	1.49	1.18	1.19	2.15	5.00	3.71	14.00	1.73	2.87	2.71	5.34	1.29	1.51	3.05	8.57	3.10	9.36
P13	2.87	4.47	1.00	1.65	0.72	0.78	0.89	1.34	1.70	4.33	5.11	6.44	1.36	3.48	1.46	3.90	0.97	0.75	3.77	5.36	4.03	4.60
P14	3.50	5.25	0.99	1.15	0.86	1.06	0.87	1.04	3.35	2.47	10.56	10.51	1.30	1.47	2.62	2.22	0.95	1.09	8.83	9.02	8.63	10.31
P15	2.85	3.23	1.02	1.08	1.20	1.44	1.05	0.84	2.02	6.55	4.88	9.86	3.64	4.06	2.08	1.09	0.89	1.08	3.86	5.75	3.82	5.09

C

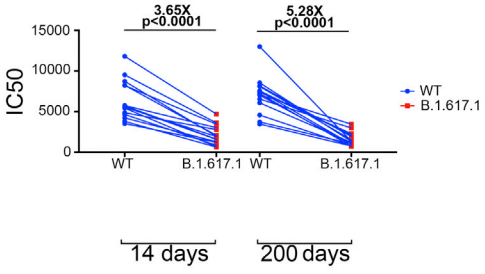

D

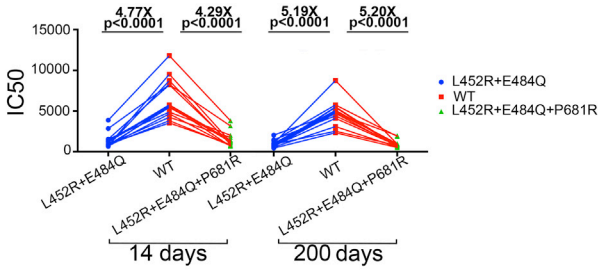

E

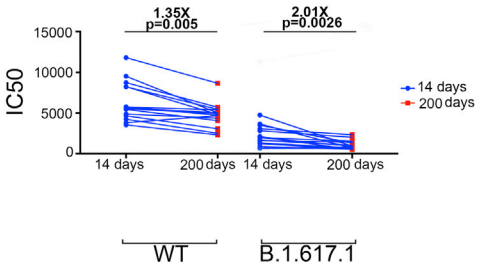

F

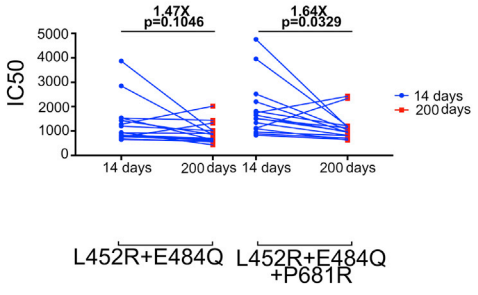

Figure 4. B.1.617.1, L452R, E484Q, L452R + E484Q, and L452R + E484Q + P681R pseudoviruses are more resistant to neutralizing antibody of convalescent sera

(A) Neutralization assay results of 15 convalescent volunteers (P01-P15) against WT and B.1.617.1 at 14 and 200 days after discharge. All data were obtained from three independent experiments (mean ± SEM). The X axis is log10, which represents the plasma dilution ratio, and the Y axis, which represents the protective efficacy of neutralizing antibodies.

(B) Ratios of IC_{50} of WT to IC_{50} of all 12 variants after 14 and 200 days represented as a heatmap with darker color implying greater change (≥2.5-fold).

(C) Change in plasma neutralization IC_{50} values of 15 convalescent volunteers from WT to B.1.617.1 at 14 and 200 days after discharge, respectively.

(D) Change in plasma neutralization IC_{50} values of 15 convalescent volunteers from WT to L452R + E484Q and L452R + E484Q + P681R at 14 days and 200 days after discharge, respectively.

(E) Change in plasma neutralization IC_{50} values of 15 convalescent volunteers at 14 and 200 days after discharge for WT and B.1.617.1, respectively.

(F) Change in plasma neutralization IC_{50} values of 28 vaccines at 14 and 200 days after discharge for L452R + E484Q and L452R + E484Q + P681R, respectively. Mean fold changes in IC_{50} values are written above the p values. Statistical analysis was performed using a paired *t*-test. $P < 0.05$ was considered statistically significant.

against the SARS-CoV-2 variants such as B.1.617.1. On the other hand, we also found that most vaccinated individuals and convalescent volunteers showed some level of neutralization resistance to the B.1.617.1 compared to WT, consistent with previous reports (Edara et al., 2021; Ferreira et al., 2021; Hoffmann et al., 2021a,2021b; Jie et al., 2021; Liu et al., 2021b). For B.1.1.529, we found that all vaccinated individuals and convalescent volunteers displayed significant immune escape, which is consistent with results reported by other groups (Dejnirattisai et al., 2022; Cao et al., 2022; Carreño et al., 2022).

Our research focus is to determine which of the B.1.617.1 mutations within the spike proteins, or their combinations, contribute to potential neutralization resistance. It is notable that the E484K mutation has emerged independently in many variants, such as P.1, P.2, B.1.351, B.1.526, B.1.525, and P3 (Baum et al., 2020; Liu et al., 2021c; Winger and Caspari, 2021). Residue 484 has mutated into a variety of amino acids under pressure of SARS-CoV-2 convalescent serum (e.g., E484A, E484G, E448D, and E484K). Intriguingly, both the E484K (Baum et al., 2020; Chen et al., 2021; Liu et al., 2021c; Wang et al., 2021b; Weisblum et al.,

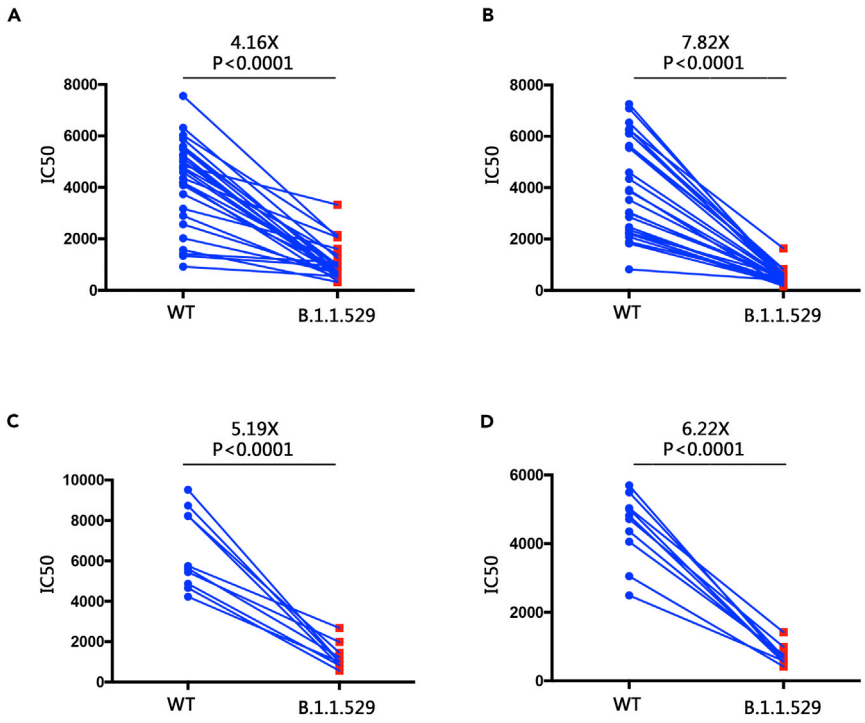

Figure 5. Neutralization efficacy of plasma from vaccines and convalescent about B.1.1.529 mutant

(A and B) Change in plasma neutralization IC_{50} values of 28 vaccines from WT to B.1.1.529 at 1 (A) and 3 months (B) after vaccination, respectively.

(C and D) Change in plasma neutralization IC_{50} values of 10 convalescent volunteers from WT to B.1.1.529 at 14 (C) and 200 days (D) after discharge, respectively.

2020) and E484Q mutations (Ferreira et al., 2021) can contribute to the resistance. All variants of B.1.617.1 harbor the E484Q mutation, further supporting that this mutation can at least partially explain the observed decreased susceptibility to neutralization by convalescent serum.

The P681R mutation in the S protein of B.1.617.1 lineage is a unique and newly identified mutation. We found that the P681R mutation facilitates furin-mediated spike cleavage and enhances syncytia formation compared to WT, which is consistent with previous reports (Weisblum et al., 2020).

In summary, we demonstrated that the B.1.617.1 variant exhibited both higher infectivity and neutralization resistance. Pseudoviruses carrying single mutations (L452R, E484Q) or double (L452R/E484Q) or triple (L452R/E484Q/P681R) mutations contribute to a potential neutralization resistance and enhanced infectivity. A major contributor to the neutralization resistance of the B.1.617.1 variant virus appears to be E484Q. Ultimately, development of new vaccines capable of eliciting broadly neutralizing antibodies may be necessary to resolve the ongoing pandemic.

STAR★METHODS

Detailed methods are provided in the online version of this paper and include the following:

- KEY RESOURCES TABLE
- RESOURCE AVAILABILITY
  - Lead contact
  - Materials availability
  - Data and code availability
- EXPERIMENTAL MODEL AND SUBJECT DETAILS
  - Bioinformatics
  - Cell culture
  - Antibody and reagents
  - Human plasma
  - Construction and production of pseudoviruses
  - Titration of pseudoviruses
  - Infection assay
  - Western Blot
  - Protein purification
  - Affinity of ACE2 and S protein
  - Flow cytometry
  - Neutralization assay
- QUANTIFICATION AND STATISTICAL ANALYSIS

SUPPLEMENTAL INFORMATION

Supplemental information can be found online at https://doi.org/10.1016/j.isci.2022.105016.

ACKNOWLEDGMENTS

This work was supported by the National Natural Science Foundation of China (82041001, 31771484, 81761128020). The funders had no roles in experimental design, data collection and analysis, interpretation of the data, or writing of this article.

AUTHOR CONTRIBUTIONS

H.Z. and H.L. conceived and designed the experiments. X.Y., Y.Z., J.X., and J.L. carried out most experiments. Q.W., Y.L., X.S., S.Y., X.Z., J.W., H.P., J.Y., L.Z., Y.L., Q.L., H.L., C.Z., L.J., and J.X. participated in some of the experiments. H.Z., H.L., J.L., D.L., X.Z., J.X., P.W., C.Y., and S.J. directed and supervised the experiments and interpretation of data. X.Y., Y.Z., S.J., and H.Z. wrote the article and approved the publication.

DECLARATION OF INTERESTS

The authors declare no competing interests.

INCLUSION AND DIVERSITY

We worked to ensure ethnic or other types of diversity in the recruitment of human subjects. We worked to ensure that the study questionnaires were prepared in an inclusive way. While citing references scientifically relevant for this work, we also actively worked to promote gender balance in our reference list. The author list of this paper includes contributors from the location where the research was conducted who participated in the data collection, design, analysis, and/or interpretation of the work.

Received: October 14, 2021
Revised: April 12, 2022
Accepted: August 19, 2022
Published: September 16, 2022

REFERENCES

Baum, A., Fulton, B.O., Wloga, E., Copin, R., Pascal, K.E., Russo, V., Giordano, S., Lanza, K., Negron, N., Ni, M., et al. (2020). Antibody cocktail to SARS-CoV-2 spike protein prevents rapid mutational escape seen with individual antibodies. Science *369*, 1014–1018. https://doi.org/10.1126/science.abd0831.

Benton, D.J., Wrobel, A.G., Xu, P., Roustan, C., Martin, S.R., Rosenthal, P.B., Skehel, J.J., and Gamblin, S.J. (2020). Receptor binding and priming of the spike protein of SARS-CoV-2 for membrane fusion. Nature *588*, 327–330. https://doi.org/10.1038/s41586-020-2772-0.

Cao, Y., Wang, J., Jian, F., Xiao, T., Song, W., Yisimayi, A., Huang, W., Li, Q., Wang, P., An, R., et al. (2022). Omicron escapes the majority of existing SARS-CoV-2 neutralizing antibodies. Nature *602*, 657–663. https://doi.org/10.1038/s41586-021-04385-3.

Carreño, J.M., Alshammary, H., Tcheou, J., Singh, G., Raskin, A.J., Kawabata, H., Sominsky, L.A., Clark, J.J., Adelsberg, D.C., Bielak, D.A., et al. (2022). Activity of convalescent and vaccine serum against SARS-CoV-2 Omicron. Nature *602*, 682–688. https://doi.org/10.1038/s41586-022-04399-5.

Cerutti, G., Guo, Y., Zhou, T., Gorman, J., Lee, M., Rapp, M., Reddem, E.R., Yu, J., Bahna, F., Bimela, J., et al. (2021). Potent SARS-CoV-2 neutralizing antibodies directed against spike N-terminal domain target a single supersite. Cell Host Microbe *29*, 819–833.e7. https://doi.org/10.1016/j.chom.2021.03.005.

Chen, R.E., Zhang, X., Case, J.B., Winkler, E.S., Liu, Y., VanBlargan, L.A., Liu, J., Errico, J.M., Xie, X., Suryadevara, N., et al. (2021). Resistance of SARS-CoV-2 variants to neutralization by monoclonal and serum-derived polyclonal antibodies. Nat. Med. *27*, 717–726. https://doi.org/10.1038/s41591-021-01294-w.

Cherian, S., Potdar, V., Jadhav, S., Yadav, P., Gupta, N., Das, M., Rakshit, P., Singh, S., Abraham, P., and Panda, S.; NIC team (2021). Convergent evolution of SARS-CoV-2 spike mutations, L452R, E484Q and P681R, in the second wave of COVID-19 in Maharashtra, India. Microorganisms *9*, 1542. https://doi.org/10.3390/microorganisms9071542.

Collier, D.A., De Marco, A., Ferreira, I.A.T.M., Meng, B., Datir, R.P., Walls, A.C., Kemp, S.A., Bassi, J., Pinto, D., Silacci-Fregni, C., et al. (2021). Sensitivity of SARS-CoV-2 B.1.1.7 to mRNA vaccine-elicited antibodies. Nature *593*, 136–141. https://doi.org/10.1038/s41586-021-03412-7.

Crawford, K.H.D., Eguia, R., Dingens, A.S., Loes, A.N., Malone, K.D., Wolf, C.R., Chu, H.Y., Tortorici, M.A., Veesler, D., Murphy, M., et al. (2020). Protocol and reagents for pseudotyping lentiviral particles with SARS-CoV-2 spike protein for neutralization assays. Viruses *12*, 513. https://doi.org/10.3390/v12050513.

Dejnirattisai, W., Huo, J., Zhou, D., Zahradník, J., Supasa, P., Liu, C., Duyvesteyn, H.M.E., Ginn, H.M., Mentzer, A.J., Tuekprakhon, A., et al. (2022). SARS-CoV-2 Omicron-B.1.1.529 leads to widespread escape from neutralizing antibody responses. Cell *185*, 467–484.e15. https://doi.org/10.1016/j.cell.2021.12.046.

Edara, V.V., Lai, L., Sahoo, M.K., Floyd, K., Sibai, M., Solis, D., Flowers, M.W., Hussaini, L., Ciric, C.R., Bechnack, S., et al. (2021). Infection and vaccine-induced neutralizing antibody responses to the SARS-CoV-2 B.1.617.1 variant. Preprint at bioRxiv. https://doi.org/10.1101/2021.05.09.443299.

Faria, N.R., Mellan, T.A., Whittaker, C., Claro, I.M., Candido, D.D.S., Mishra, S., Crispim, M.A.E., Sales, F.C., Hawryluk, I., McCrone, J.T., et al. (2021). Genomics and epidemiology of a novel SARS-CoV-2 lineage in Manaus. Preprint at medRxiv. https://doi.org/10.1101/2021.02.26.21252554.

Ferreira, I., Datir, R., Papa, G., Kemp, S., and Gupta, R.K. (2021). SARS-CoV-2 B.1.617 emergence and sensitivity to vaccine-elicited antibodies. Preprint at BioRxiv. https://doi.org/10.1101/2021.05.08.443253.

Galloway, S.E., Paul, P., MacCannell, D.R., Johansson, M.A., Brooks, J.T., MacNeil, A., Slayton, R.B., Tong, S., Silk, B.J., Armstrong, G.L., et al. (2021). Emergence of SARS-CoV-2 B.1.1.7 lineage - United States, december 29, 2020-january 12, 2021. MMWR Morb. Mortal. Wkly. Rep. *70*, 95–99. https://doi.org/10.15585/mmwr.mm7003e2.

Garcia-Beltran, W.F., Lam, E.C., St Denis, K., Nitido, A.D., Garcia, Z.H., Hauser, B.M., Feldman, J., Pavlovic, M.N., Gregory, D.J., Poznansky, M.C., et al. (2021). Multiple SARS-CoV-2 variants escape neutralization by vaccine-induced humoral immunity. Cell *184*, 2372–2383.e9. https://doi.org/10.1016/j.cell.2021.03.013.

Gupta, R.K. (2021). Will SARS-CoV-2 variants of concern affect the promise of vaccines? Nat. Rev. Immunol. *21*, 340–341. https://doi.org/10.1038/s41577-021-00556-5.

Harvey, W.T., Carabelli, A.M., Jackson, B., Gupta, R.K., Thomson, E.C., Harrison, E.M., Ludden, C., Reeve, R., Rambaut, A., et al.; COVID-19 Genomics UK COG-UK Consortium (2021). SARS-CoV-2 variants, spike mutations and immune escape. Nat. Rev. Microbiol. *19*, 409–424. https://doi.org/10.1038/s41579-021-00573-0.

Hoffmann, M., Arora, P., Groß, R., Seidel, A., Hörnich, B.F., Hahn, A.S., Krüger, N., Graichen, L., Hofmann-Winkler, H., Kempf, A., et al. (2021a). SARS-CoV-2 variants B.1.351 and P.1 escape from neutralizing antibodies. Cell *184*, 2384–2393.e12. https://doi.org/10.1016/j.cell.2021.03.036.

Hoffmann, M., Hofmann-Winkler, H., Krüger, N., Kempf, A., Nehlmeier, I., Graichen, L., Arora, P., Sidarovich, A., Moldenhauer, A.S., Winkler, M.S., et al. (2021b). SARS-CoV-2 variant B.1.617 is resistant to Bamlanivimab and evades antibodies induced by infection and vaccination. Cell Rep. *36*, 109415. https://doi.org/10.1016/j.celrep.2021.109415.

Hyseni, I., Molesti, E., Benincasa, L., Piu, P., Casa, E., Temperton, N.J., Manenti, A., and Montomoli, E. (2020). Characterisation of SARS-CoV-2 lentiviral pseudotypes and correlation between pseudotype-based neutralisation assays and live virus-based micro neutralisation assays. Viruses *12*, 1011. https://doi.org/10.3390/v12091011.

Jie, H., Xiao-yu, W., Jin, X., Pai, P., Feng-li, X., Kang, W., Fei-yang, L., Ai-shun, J., Liang, F., Bei-zhong, L., et al. (2021). Reduced neutralization of SARS-CoV-2 B.1.617 variant by inactivated and RBD-subunit vaccine. Preprint at bioRxiv. https://doi.org/10.1101/2021.07.09.451732.

Leung, K., Shum, M.H., Leung, G.M., Lam, T.T., and Wu, J.T. (2021). Early transmissibility assessment of the N501Y mutant strains of SARS-CoV-2 in the United Kingdom, October to November 2020. Euro Surveill. *26*, 2002106. https://doi.org/10.2807/1560-7917.ES.2020.26.1.2002106.

Liu, J., Liu, Y., Xia, H., Zou, J., Weaver, S.C., Swanson, K.A., Cai, H., Cutler, M., Cooper, D., Muik, A., et al. (2021a). BNT162b2-elicited neutralization of B.1.617 and other SARS-CoV-2 variants. Nature *596*, 273–275. https://doi.org/10.1038/s41586-021-03693-y.

Liu, Y., Liu, J., Xia, H., Zhang, X., Fontes-Garfias, C.R., Swanson, K.A., Cai, H., Sarkar, R., Chen, W., Cutler, M., et al. (2021b). Neutralizing activity of BNT162b2-elicited serum. N. Engl. J. Med. *384*, 1466–1468. https://doi.org/10.1056/NEJMc2102017.

Liu, Z., VanBlargan, L.A., Bloyet, L.M., Rothlauf, P.W., Chen, R.E., Stumpf, S., Zhao, H., Errico, J.M., Theel, E.S., Liebeskind, M.J., et al. (2021c). Identification of SARS-CoV-2 spike mutations that attenuate monoclonal and serum antibody neutralization. Cell Host Microbe *29*, 477–488.e4. https://doi.org/10.1016/j.chom.2021.01.014.

McCallum, M., De Marco, A., Lempp, F.A., Tortorici, M.A., Pinto, D., Walls, A.C., Beltramello, M., Chen, A., Liu, Z., Zatta, F., et al. (2021). N-terminal domain antigenic mapping reveals a site of vulnerability for SARS-CoV-2. Cell *184*, 2332–2347.e16. https://doi.org/10.1016/j.cell.2021.03.028.

Mlcochova, P., Kemp, S.A., Dhar, M.S., Papa, G., Meng, B., Ferreira, I.A.T.M., Datir, R., Collier, D.A., Albecka, A., Singh, S., et al. (2021). SARS-CoV-2 B.1.617.2 Delta variant replication and immune evasion. Nature *599*, 114–119. https://doi.org/10.1038/s41586-021-03944-y.

Nelson, G., Buzko, O., Spilman, P., Niazi, K., Rabizadeh, S., and Soon-shiong, P. (2021). Molecular dynamic simulation reveals E484K mutation enhances spike RBD-ACE2 affinity and the combination of E484K, K417N and N501Y mutations (501Y. V2 variant) induces conformational change greater than N501Y mutant alone, potentially resulting in an escape mutant. Preprint at bioRxiv. https://doi.org/10.1101/2021.01.13.426558.

Piccoli, L., Park, Y.J., Tortorici, M.A., Czudnochowski, N., Walls, A.C., Beltramello, M., Silacci-Fregni, C., Pinto, D., Rosen, L.E., Bowen, J.E., et al. (2020). Mapping neutralizing and immunodominant sites on the SARS-CoV-2 spike receptor-binding domain by structure-guided high-resolution serology. Cell *183*, 1024–1042.e21. https://doi.org/10.1016/j.cell.2020.09.037.

Rambaut, A., Holmes, E.C., O'Toole, Á., Hill, V., McCrone, J.T., Ruis, C., du Plessis, L., and Pybus, O.G. (2020). A dynamic nomenclature proposal for SARS-CoV-2 lineages to assist genomic epidemiology. Nat. Microbiol. *5*, 1403–1407. https://doi.org/10.1038/s41564-020-0770-5.

Tan, C.W., Chia, W.N., Qin, X., Liu, P., Chen, M.I.C., Tiu, C., Hu, Z., Chen, V.C.W., Young, B.E., Sia, W.R., et al. (2020). A SARS-CoV-2 surrogate virus neutralization test based on antibody-mediated blockage of ACE2-spike protein-protein interaction. Nat. Biotechnol. *38*, 1073–1078. https://doi.org/10.1038/s41587-020-0631-z.

Tegally, H., Wilkinson, E., Giovanetti, M., Iranzadeh, A., Fonseca, V., Giandhari, J., Doolabh, D., Pillay, S., San, E.J., Msoni, N., et al. (2020). Emergence and rapid spread of a new severe acute respiratory syndrome-related coronavirus 2 (SARS-CoV-2) lineage with multiple spike mutations in South Africa. Preprint at medRxiv. https://doi.org/10.1101/2020.12.21.20248640.

Tegally, H., Wilkinson, E., Giovanetti, M., Iranzadeh, A., Fonseca, V., Giandhari, J., Doolabh, D., Pillay, S., San, E.J., Msomi, N., et al. (2021). Detection of a SARS-CoV-2 variant of concern in South Africa. Nature *592*, 438–443. https://doi.org/10.1038/s41586-021-03402-9.

Trifinopoulos, J., Nguyen, L.T., von Haeseler, A., and Minh, B.Q. (2016). W-IQ-TREE: a fast online phylogenetic tool for maximum likelihood analysis. Nucleic Acids Res. *44*, W232–W235. https://doi.org/10.1093/nar/gkw256.

Volz, E., Hill, V., McCrone, J.T., Price, A., Jorgensen, D., O'Toole, Á., Southgate, J., Johnson, R., Jackson, B., Nascimento, F.F., et al. (2021a). Evaluating the effects of SARS-CoV-2 spike mutation D614G on transmissibility and pathogenicity. Cell *184*, 64–75.e11. https://doi.org/10.1016/j.cell.2020.11.020.

Volz, E., Mishra, S., Chand, M., Barrett, J.C., Johnson, R., Geidelberg, L., Hinsley, W.R., Laydon, D.J., Dabrera, G., O'Toole, Á., et al. (2021b). Assessing transmissibility of SARS-CoV-2 lineage B.1.1.7 in England. Nature *593*, 266–269. https://doi.org/10.1038/s41586-021-03470-x.

Wang, P., Casner, R.G., Nair, M.S., Wang, M., Yu, J., Cerutti, G., Liu, L., Kwong, P.D., Huang, Y., Shapiro, L., and Ho, D.D. (2021a). Increased resistance of SARS-CoV-2 variant P.1 to antibody neutralization. Cell Host Microbe *29*, 747–751.e4. https://doi.org/10.1016/j.chom.2021.04.007.

Wang, P., Nair, M.S., Liu, L., Iketani, S., Luo, Y., Guo, Y., Wang, M., Yu, J., Zhang, B., Kwong, P.D., et al. (2021b). Antibody resistance of SARS-CoV-2 variants B.1.351 and B.1.1.7. Nature *593*, 130–135. https://doi.org/10.1038/s41586-021-03398-2.

Wang, Q., Zhang, Y., Wu, L., Niu, S., Song, C., Zhang, Z., Lu, G., Qiao, C., Hu, Y., Yuen, K.Y., et al. (2020). Structural and functional basis of SARS-CoV-2 entry by using human ACE2. Cell *181*, 894–904.e9. https://doi.org/10.1016/j.cell.2020.03.045.

Weisblum, Y., Schmidt, F., Zhang, F., DaSilva, J., Poston, D., Lorenzi, J.C., Muecksch, F., Rutkowska, M., Hoffmann, H.H., Michailidis, E., et al. (2020). Escape from neutralizing antibodies by SARS-CoV-2 spike protein variants. Elife *9*, e61312. https://doi.org/10.7554/eLife.61312.

Winger, A., and Caspari, T. (2021). The spike of concern—the novel variants of SARS-CoV-2. Viruses *13*, 1002. https://doi.org/10.3390/v13061002.

Wise, J. (2021). Covid-19: the E484K mutation and the risks it poses. BMJ *372*, n359. https://doi.org/10.1136/bmj.n359.

Wu, F., Zhao, S., Yu, B., Chen, Y.M., Wang, W., Song, Z.G., Hu, Y., Tao, Z.W., Tian, J.H., Pei, Y.Y., et al. (2020). A new coronavirus associated with human respiratory disease in China. Nature *579*, 265–269. https://doi.org/10.1038/s41586-020-2008-3.

Wu, K., Werner, A.P., Moliva, J.I., Koch, M., Choi, A., Stewart-Jones, G.B.E., Bennett, H., Boyoglu-Barnum, S., Shi, W., Graham, B.S., et al. (2021). mRNA-1273 vaccine induces neutralizing antibodies against spike mutants from global SARS-CoV-2 variants. Preprint at bioRxiv. https://doi.org/10.1101/2021.01.25.427948.

Zhou, D., Dejnirattisai, W., Supasa, P., Liu, C., Mentzer, A.J., Ginn, H.M., Zhao, Y., Duyvesteyn, H.M.E., Tuekprakhon, A., Nutalai, R., et al. (2021). Evidence of escape of SARS-CoV-2 variant B.1.351 from natural and vaccine-induced sera. Cell *184*, 2348–2361.e6. https://doi.org/10.1016/j.cell.2021.02.037.

Zhou, P., Yang, X.L., Wang, X.G., Hu, B., Zhang, L., Zhang, W., Si, H.R., Zhu, Y., Li, B., Huang, C.L., et al. (2020). A pneumonia outbreak associated with a new coronavirus of probable bat origin. Nature *579*, 270–273. https://doi.org/10.1038/s41586-020-2012-7.

STAR★METHODS

KEY RESOURCES TABLE

REAGENT or RESOURCE	SOURCE	IDENTIFIER
Antibodies		
HA antibody	Cell Signaling Technology	Cat.#:3724; RRID:AB_1549585
goat anti-mouse IgG(H + L) HRP	Beyotime	Cat.#:A0216; RRID:AB_2860575
HIV-1 p24 antibody	Abcam	Cat.#:ab63958; RRID:AB_1139522
Flag antibody	Cell Signaling Technology	Cat.#:8146; RRID:AB_10950495
Chemicals		
2 × Taq Master Mix	Vazyme	Cat.#:P112
High fidelity PCR enzyme- 2 × Phanta Max Master Mix	Vazyme	Cat.#:P515
DMEM	HyClone	Cat.#:SH300243.01
Fetal Bovine Sera	ExCell Bio	Cat.#:FSP500
Penicillin/streptomycin	Gibco	Cat.#:151140163
0.25% Trypsin-EDTA	Gibco	Cat.#:25200072
Critical commercial assays		
luciferase detection kit	Yeasen	Cat.#:11407ES80
HIV-1 Gag P24 kit	R&D	Cat.#:7360-05
Experimental models: Cell lines		
HEK293T/17	ATCC	Cat.#:CRL-3216
Huh-7	CCLV	Cat.#:RIE 1079
Calu-3	ATCC	Cat.#:HTB-55 BCRJ
293T-hACE2	This paper	N/A
Recombinant DNA		
pLenti.GFP.NLuc	This paper	N/A
psPAX2	addgene	Cat.#:12260
pcDNA3.1-B.1.617.1	This paper	N/A
pcDNA3.1-B.1.1.529	This paper	N/A
Software		
FlowJo Version 10.0	Tree Star	https://www.flowjo.com/
ImageLab software	Bio-rad	N/A
GraphPad Prism V7.0	GraphPad	https://www.graphpad.com

RESOURCE AVAILABILITY

Lead contact

Further information and requests for resources and reagents should be directed to and will be fulfilled by the lead contact, Professor Huanzhang Zhu (hzzhu@fudan.edu.cn).

Materials availability

These unique reagents will be made available upon request.

Data and code availability

Data reported in this paper will be shared by the lead contact upon request. This paper does not report original code. Any additional information required to reanalyze the data reported in this paper is available from the lead contact upon request.

EXPERIMENTAL MODEL AND SUBJECT DETAILS

Bioinformatics

200 SARS-CoV-2 whole genome sequences with related lineage information downloaded from NCBI VIRUS (https://www.ncbi.nlm.nih.gov/labs/virus) were aligned using alignment tools of NCBI, and a Maximum Likelihood phylogenetic tree was constructed using the IQ-TREE Web Server (http://iqtree.cibiv.univie.ac.at/) (Trifinopoulos et al., 2016), employing GTR as the substitution model and 1,000 bootstrap replications.

Mutation analysis for all genomes was done using CoVsurver: Mutation Analysis of hCoV-19 (https://www.gisaid.org/epiflu-applications/covsurver-mutations-app/). The frequency of each lineage's nonsynonymous mutations was calculated by considering SARS-CoV-2 isolate WuhanHu-1 as the reference strain.

Several top mutations in the S protein, the crystal structure of which was complexed with ACE2, were obtained from the protein data bank (PDB ID: 7A98) (Benton et al., 2020) and mapped using Biovia Discovery studio visualizer 2020.The crystal structure of SARS-CoV-2 spike RBD domain complexed with ACE2(PDB ID: 6LZG) (Cherian et al., 2021; Wang et al., 2020) was implemented.

Cell culture

HEK293T/17 and Calu-3 cell lines were purchased from ATCC, Huh-7was purchased from CCLV, and the 293T-hACE2 cell line was generated by our lab. These cells all were cultured in Dulbecco's Modified Eagle's Medium (DMEM, HyClone, SH300243.01) with 10% Fetal Bovine Sera (FBS, ExCell Bio, FSP500) and 1% penicillin/streptomycin (Gibco, 151140163) in a 37°C incubator containing 5% CO2. 0.25% Trypsin-EDTA (Gibco, 25200072) was used to digest cells for subculture.

Antibody and reagents

The following antibodies were used throughout this study: from Cell Signaling Technology (MA, USA), anti-HA (3427), anti-Flag(8416), from Abcam (MA, USA), anti-HIV-1 p24 (ab63958), and from Beyotime (Shanghai, China), goat anti-mouse lgG(H + L) HRP (A0216). 2 × Taq Master Mix (P112) and High fidelity PCR enzyme-2 × Phanta Max Master Mix (P515) were purchased from Vazyme (Nanjing, China). Plasmid Extraction Kits (DP103, DP108, DP117) were purchased from Tiangen (Beijing, China). The luciferase detection kit (11407ES80) was purchased from Yeasen (Shanghai, China).

Human plasma

This study was approved by the Ethics Committee of Shanghai Public Health Clinical Center and Fudan University. Human plasma samples were collected from 15 COVID-19 convalescent volunteers which were infected with wild-type Wuhan strains at the Shanghai Municipal Public Health Center and 28 BBIBP-CorV vaccines from Fudan University. Each volunteer underwent a total of two rounds of blood sampling. For vaccines, the first blood sample was taken after the second inoculation. The second blood sample was taken three months after the vaccination was complete. For COVID-19 convalescent volunteers, the interval of blood sampling was performed at two follow-up visits after discharge. The first interval was nearly15 days, and the second interval was nearly 200 days. The detailed information of volunteers is listed in Table 1.

Construction and production of pseudoviruses

The spike of SARS-CoV-2 and that of all variant plasmids were synthesized by the GeneScript Company. All S proteins were optimized with 18 amino acids removed and an HA tag attached. The core plasmid, pLenti.GFP.NLuc, that expresses GFP and luciferase at the same time was maintained in our laboratory.

For production of pseudoviruses, HEK293T/17 cells were seeded into 10cm dishes one day before transfection. When the cells reached 80% confluence, plasmid and PEI were added into the Opti-MDM (Gibco), mixed evenly, and left standing for 20 min pLenti.GFP.NLuc, psPAX2 and the S protein vector were co-transfected into HEK293T/17 cells to produce the pseudoviruses. After incubation at 37°C and 5% CO2 for 24h, the culture medium was changed with DMEM with 2% FBS and 1% P/S. The supernatants containing SARS-CoV-2 pseudotyped viruses were harvested at 48 and 72h after transfection and filtered by 0.45μm pore size. The filtrates were centrifuged at 25000rpm and 4°C for 2h. The supernatants were

discarded, and the pseudovirus stocks were dissolved in DMEM for storage at −80°C (Crawford et al., 2020; Hyseni et al., 2020; Tan et al., 2020).

Titration of pseudoviruses

The HIV-1 Gag P24 kit (R&D, 7360-05) was used to detect the titration of pseudoviruses (Crawford et al., 2020). Briefly, the capture antibody was diluted to the working concentration in PBS. A 96-well plate was coated with 100ul per well of the antibody. The plate was sealed and incubated overnight at room temperature. The 96-well plate was washed by wash buffer 3 times. 300 ul of reagent diluent were added to each well to block the plate and then incubated at room temperature for 1h. The plate was then washed as the last step. The standards and detection antibody diluted in reagent diluent were added to each well and incubated for 2 h at room temperature. The wells were washed 3 times. 100ul of the working dilution of streptavidin-HRP were added to each well. After incubation for 20 min at room temperature, the plate was washed again. With the substrate added to each well, the titrations of pseudoviruses were calculated in GraphPad Prism (Crawford et al., 2020).

Infection assay

To measure the infectivity of pseudoviruses (Hyseni et al., 2020), 1 μL (MOI = 0.1) of the pseudoviruses was added to a 96-well plate and seeded at 10^4 cells per well in 100 μL culture medium at 37°C, 5% CO2. After 12–16 h, the culture medium was refreshed, and cells were incubated for an additional 48 h, followed by photographing and harvesting for the luciferase reporter gene experiment. Briefly, cells were harvested at 72 h post-infection, and the lysate was assayed for luciferase activity. Triplicate cultures were measured for each experiment.

Western Blot

20 μL pseudoviruses were harvested, lysed, subjected to SDS PAGE, and then transferred onto nitrocellulose filter (NC) membrane, followed by incubation with indicated primary antibody. Membranes were visualized using the Immun-Star Western Chemiluminescence Kit (Bio-Rad). Images were captured using a ChemiDoc XRS + System and processed using ImageLab software (Bio-Rad).

Protein purification

The S protein of SARS-CoV-2 pseudoviruses was produced in HEK 293T cells. After the plasmid of S protein was transfected for 48 h, the cells were collected and lysed. Anti-HA protein A/G magnetic beads were then used for immunoprecipitation and quantified by BCA kit.

Affinity of ACE2 and S protein

ELISA was used to detect the affinity of ACE2 and S protein (Tan et al., 2020). The plate was coated with 100 μL per well of ACE2 protein (Novoprotein, C419). The plate was sealed and incubated overnight at room temperature. After blocking, the plate was incubated at room temperature for 1 h. The purified S protein diluted in reagent diluent was added and incubated for 2 h. After washing, 100 μL of the working dilution of anti-HA were added to each well. Another incubation was performed for 2 h in which goat anti-mouse IgG HRP was combined with anti-HA to reveal the affinity of ACE2 and S protein with the addition of substrate.

Flow cytometry

All the cells were washed, resuspended in 100 μL PBS containing specific antibodies and incubated for 30 min at 4°C. Data were acquired on a Beckman Coulter Gallios flow cytometer and analyzed by FlowJo version 10 (Tree Star, Ashland, OR).

Neutralization assay

A total of 100ul 293T-hACE2 cells were seeded in a 96-well plate at a concentration of 1×10^5/mL cells (1×10^4 cells per well) and cultured for 12 h. Briefly, each plasma was 10-fold serially diluted with 10% FBS in DMEM after the first dilution of 1:40. The pseudoviruses with concentration of MOI = 0.25 were added to 100 μL serial dilutions of plasma and incubated at 37°C for 30 min. The mixture was added to cultured cells. The culture medium was refreshed after 24 h and incubated for an additional 48 h. Chemiluminescence was measured by luciferase assay kit (Chen et al., 2021). Each dilution has 3 duplicates. The IC_{50} values were calculated by a three-parameter dose-response inhibition curve in GraphPad Prism 8.

QUANTIFICATION AND STATISTICAL ANALYSIS

GraphPad Prism 8 was used for drawing plots and statistical analysis. Volunteer information was represented by the median. T-test was used to analyze the difference between each group. Nonlinear regression was applied to calculate the IC_{50}. When the p value was less than 0.05, it was considered to be a statistically significant difference. *p represented p value less than 0.05; **p represented p value less than 0.005; ***p represented p value less than 0.0005; ns represented no significant difference between each group.